ISABE-2011-1340

Turboelectric Distributed Propulsion in a Hybrid Wing Body Aircraft

James L. Felder, Gerald V. Brown, Hyun Dae Kim
NASA Glenn Research Center
Cleveland, Ohio 44135 USA

Julio Chu
NASA Langley Research Center
Hampton, Virginia, 23681, USA

Abstract

The performance of the N3-X, a 300 passenger hybrid wing body (HWB) aircraft with turboelectric distributed propulsion (TeDP), has been analyzed to see if it can meet the 70% fuel burn reduction goal of the NASA Subsonic Fixed Wing project for N+3 generation aircraft. The TeDP system utilizes superconducting electric generators, motors and transmission lines to allow the power producing and thrust producing portions of the system to be widely separated. It also allows a small number of large turboshaft engines to drive any number of propulsors. On the N3-X these new degrees of freedom were used to (1) place two large turboshaft engines driving generators in freestream conditions to maximize thermal efficiency and (2) to embed a broad continuous array of 15 motor driven propulsors on the upper surface of the aircraft near the trailing edge. That location maximizes the amount of the boundary layer ingested and thus maximizes propulsive efficiency. The Boeing B777-200LR flying 7500 nm (13890 km) with a cruise speed of Mach 0.84 and an 118100 lb payload was selected as the reference aircraft and mission for this study. In order to distinguish between improvements due to technology and aircraft configuration changes from those due to the propulsion configuration changes, an intermediate configuration was included in this study. In this configuration a pylon mounted, ultra high bypass (UHB) geared turbofan engine with identical propulsion technology was integrated into the same hybrid wing body airframe. That aircraft achieved a 52% reduction in mission fuel burn relative to the reference aircraft. The N3-X was able to achieve a reduction of 70% and 72% (depending on the cooling system) relative to the reference aircraft. The additional 18% - 20% reduction in the mission fuel burn can therefore be attributed to the additional degrees of freedom in the propulsion system configuration afforded by the TeDP system that eliminates nacelle and pylon drag, maximizes boundary layer ingestion (BLI) to reduce inlet drag on the propulsion system, and reduces the wake drag of the vehicle.

Nomenclature

A	area
AC	alternating current
ADP	aerodynamic design point
BLI	boundary layer ingestion
BSSCO	bismuth strontium calcium copper oxide
CAEP	Committee on Aviation Environmental Protection
C_{dth}	nozzle throat discharge coefficient
C_V	nozzle velocity coefficient
DC	direct current
FPR	Fan Pressure Ratio
HWB	hybrid-wing-body
ISA	International Standard Atmosphere
LTO	landing and take-off

K	Kelvins
M	Mach number
MgB_2	magnesium di-boride
MIT	Massachusetts Institute of Technology
NRA	NASA Research Announcements
NOx	oxides of nitrogen
nm	nautical mile
P	pressure
R	degrees Rankine
RTO	rolling take-off
TeDP	turboelectric distributed propulsion
UHB	ulta-high bypass
YBCO	yttrium barium copper oxide

Introduction

The NASA Subsonic Fixed Wing (SFW) project has defined goals for the next three generations of aircraft in four key areas of reducing noise, fuel burn, emissions and field length. Table 1outlines goals for each generation. The dates given for each generation are targets for attaining technology readiness levels (TRL) 4 to 6[1]. The NASA SFW project formed six teams, two internal and four external, to examine concepts to meet the N+3 goals. The external teams selected during the NASA Research Announcement (NRA) phase 1 study were led by the Massachusetts Institute of Technology (MIT)[2], Northrop Grumman[3], Boeing[4] and General Electric (GE)[5]. Northrop Grumman, Boeing and MIT examined medium size and range aircraft in the 150 passenger class. MIT also examined a large intercontinental 300 passenger hybrid wing body (HWB) aircraft. The team led by GE elected to examine short range 20 passenger aircraft flying point to point between the thousands of smaller airports distributed broadly around the United States.

A NASA internal team composed of the authors felt that a radical departure in both aircraft and propulsion system was needed to meet the N+3 goals. An intercontinental mission of 7500 nm (13890 km) with a cruise speed of Mach 0.84 and a 118100 lb payload was selected as the reference mission for this study. The 300 passenger Boeing B777-200LR was selected as the reference aircraft against which to compare mission fuel burn. A reference model patterned after the B777-200LR was constructed using the NASA Flight Optimization System (FLOPS) code[6]. The predicted fuel burn from FLOPS for the reference aircraft/engine combination flying the reference mission is the value against which candidate aircraft/engine mission fuel burns are compared.

The B777-200LR is powered by the GE90-115B engine. A reference model of an engine patterned after the GE90-115B was constructed using the Numerical Propulsion System

CORNERS OF THE TRADE SPACE	N+1 (2015)*** Technology Benefits Relative to a Single Aisle Reference Configuration	N+2 (2020)*** Technology Benefits Relative to a Large Twin Aisle Reference Configuration	N+3 (2025)*** Technology Benefits
Noise (cum below Stage 4)	- 32 dB	- 42 dB	- 71 dB
LTO NOx Emissions (below CAEP 6)	-60%	-75%	better than -75%
Performance Aircraft Fuel Burn	-33%**	-50%**	better than -70%
Performance Field Length	-33%	-50%	exploit metroplex* concepts

*** Technology Readiness Level for key technologies = 4-6
** Additional gains may be possible through operational improvements
* Concepts that enable optimal use of runways at multiple airports within the metropolitan areas

Table 1 NASA Subsonic Fixed Wing Goals for the Next Three Aircraft Generations

Simulation (NPSS) code[7]. The NPSS model is labeled as the Pax300.

An HWB configuration was selected for the new aircraft. The HWB type aircraft presents an opportunity to reduce both fuel burn and aircraft noise. HWB aircraft present a relatively good lift to drag ratio (L/D) of around 22[8], leading to reduced fuel burn. The engines can be mounted on the upper aft portion of the center body where the fuselage can potentially provide noise shielding[9]. However, placing the engines on top of the fuselage presents a number of challenges.

For pylon mounted turbofans these challenges include a high thrust line relative to the aircraft center of gravity. Another challenge is either a high inlet Mach number (if the engines are sufficiently far forward to provide fuselage shielding of the exhaust noise) or loss of fuselage noise shielding (if the engines are moved aft to avoid the high velocity portions of the center wing-body). Embedding the engines into the upper aircraft surfaces addresses the high thrust center while also eliminating the weight and drag of the pylon and a portion of the nacelle. Embedded engines can also significantly reduce fuel burn by ingesting the boundary layer. Ingesting the boundary layer reduces the average inlet velocity to less than the freestream value and thus reduces the drag of the inlet. If the inlets can also be located far aft on the HWB center body airfoil section, the natural diffusion of the airfoil will also reduce the velocity of air above the boundary layer. This further reduces inlet drag for inlets that project above the boundary layer height. However, ingesting the boundary layer can result in significant losses. As documented by Tillman[10], it is easy for the losses associated with boundary layer ingestion (BLI) to more than off-set the gains.

To maximize gains while minimizing losses, the optimal BLI propulsion system on a HWB aircraft would have the following attributes:

- Inlets that ingest a large percentage of the upper surface boundary layer.
- Inlets located near the trailing edge to take full advantage of BLI and aft airfoil diffusion to reduce inlet velocity. Ideally, this would be done without causing the nozzles to project beyond the trailing edge for noise reduction reasons.
- Continuous inlets and nozzles to minimize external wetted area and avoid additional drag due to channel flow between closely spaced nacelles.
- Core engines that do not ingest the boundary layer in order to avoid losing thermal efficiency.
- A minimum number of core engines to maximize thermal efficiency due to larger turbomachinery. The ideal would be only two core engines which provide the minimum for engine-out redundancy.
- A power distribution method with high transmission efficiency.

A number of recent studies [2, 10, 12, 13] have examined the use of single-fan and multi-fan turbine engines embedded in the upper surface of an HWB aircraft. The predicted fuel burn reductions due to BLI have been in the 3%-7% range compared to a pylon mounted engine of equal technology level. Single fan turbofans require heavy, high-aspect-ratio inlets if a significant portion of the boundary layer is to be ingested and if the number of engines is limited to two or three. Performance losses due to additional internal pressure loss and additional inlet distortion can more than off-set the gains due to BLI. Low aspect ratio inlets avoid the losses of high aspect ratio inlets, but also limit the amount of boundary layer ingested, resulting in only small improvements in fuel burn. Increasing the number of engines allows the use of more low-aspect ratio inlet to ingest the same percentage of the boundary layer. However, smaller engines may be limited to lower overall pressure ratios (OPR) than larger engines and they are more susceptible to adverse effects like tip clearance and surface finish, all of which reduce thermal efficiency.

The multi-fan approach where a single core engine drives multiple fans either through mechanical, hydraulic or hot gas power

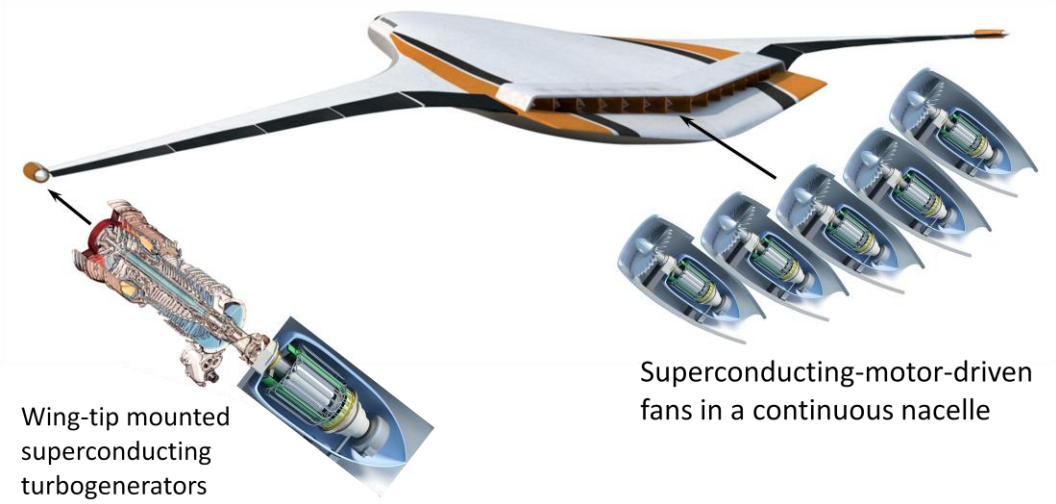

Figure 1 N3-X Hybrid Wing Body(HWB) Aircraft with a Turboelectric Distributed Propulsion (TeDP)

distribution addresses some of the issues seen with single-fan configurations, while adding some of its own. The larger number of smaller fans allows more of the boundary layer to be ingested by low aspect ratio inlets while maintaining the thermal efficiency of a few larger core engines. This approach, however adds the weight and losses of a right-angle drive gearbox, hot gas ducting or hydraulic pumps and motors. The predicted results of the multi-fan approach have ranged from a small decrease to a small increase in fuel burn relative to the standard pylon mounted engine of equal technology level.

The authors of this paper elected to examine the use of electrical energy to transmit power from the gas turbines to the fans. Transmitting all power between the turbines and the fans as electricity allows the power generator and the propulsors to be placed anywhere on the vehicle to optimize overall system performance. Electrical power can be transmitted long distances with very little loss. The flexibility in distributing electrical power allows the number of power producing devices and the number of thrust producing devices to be independent of one another. Distributing the power as direct current (DC) allows the speeds in the different devices to be independent of each other, essentially forming a infinitely variable ratio transmission between the power turbines and the fans. Also electrical power from multiple devices can be readily mixed, allowing a degree of cross connection that is very difficult to achieve with mechanical power distribution. Where other embedded engine concepts meet some of the criteria, we feel our design meets all of the criteria outlined above for an optimum BLI system.

Configuration and Assumptions

The turboelectric distributed propulsion (TeDP) system illustrated in Figure 1 consists of two turbogenerators consisting of a turboshaft engine driving superconducting electrical generator. The primary function of these devices is to make electricity, not thrust. The nozzle of the turbogenerator is sized so that there is enough jet velocity at cruise to produce a small amount of net thrust to avoid being a source of drag. They are located on the wingtips so that the inlets ingest freestream air. Most of the energy of the gas stream is extracted by the power turbine to drive the generator. As a result the exhaust velocity is low which should result in low jet noise as well. The wingtip location will also give

some bending moment relief in the normal direction at the cost of an increase in bump loading and possible aeroelasticity considerations.

There are other potential benefits of locating the turbogenerators on the wingtips. Research conducted in 1970 at NASA[11] identified reductions in induced drag of up to 40% if a thrust producing device is located at the wing tip. This reduction is due the higher velocity thrust stream reducing the strength of the wing-tip vortex well downstream of the wing itself. While the aspect ratio of the wing and the flow rate of the turbogenerators is different than the configuration tested in the wind tunnel, the basics of the configuration are the same and so there should be some induced drag reduction Another argument for the wingtip location is that it nearly eliminates the risk to the rest of the aircraft and passengers in the event of a turbine disk burst. Future analysis will further quantify these effects. The wingtip location is not mandatory. The turbogenerators can be embedded in the wing root area with a leading edge inlet or on short pylons on top of the wing if needed without sacrificing high inlet pressure recovery or incurring large installation losses.

The electric power from the turbogenerators is distributed along redundant superconducting electrical cables to an array of superconducting motor driven fans in a continuous array of propulsors spanning the entire upper trailing edge of the center wing-body section. The width of the array is set to cover all of the long chord portions of the fuselage and wing root. This maximizes the amount of boundary layer ingested as measured by the swept area ahead of the propulsors with a minimum number of propulsors.

The number of propulsors is not set, but rather is a function of the width of the array, the fan pressure ratio (FPR) and the net thrust that is required. For a given FPR, 1.3 for this study, and a given amount of thrust required by the aircraft the aggregate area of all the fans can be calculated. The number of fans, and thus propulsors, is then determined by the number of circular fans of the required aggregate area that will fit across the given array width with at least a minimum specified separation between fans.

The requirement that the propulsor array be continuous sets the width of each individual propulsor inlet to equal the total width of the array divided by the number of propulsors. The inlet height is determined by using the relationship between mass-averaged Mach number versus height above the fuselage for the specific aircraft shape and percent chord location to determine the inlet height. The mass-average Mach number and density determine the mass flow into an inlet of the given height. The height of the inlet is iterated and the mass-average Mach number reevaluated at each height until the height is such that the inlet mass flow equal to the fan mass flow. This iterative calculation is done as part of the design point calculations in the NPSS model of the TeDP system. And lastly the nozzle height is determined from the calculated nozzle area divided by the array width.

Each propulsor in the array consists only of a low aspect ratio two-dimensional (2-D) slot inlet, a fan, a short duct around the motor and a low aspect ratio 2-D slot nozzle. The result is a very short axial length for each propulsor. This allows the inlets to be located further aft to maximize BLI benefits while still allowing the nozzle to be located forward of the trailing edge. Thus fuselage noise shielding of the propulsor stream is maintained. This also means that the propulsion system does not cover the pitch effector and thus requiring thrust vectoring of the engines to control aircraft pitch.

An HWB aircraft derived from the Boeing N2A& N2B[12] and SAI SAX-40[13] with the addition of aircraft technologies anticipated to be available in the N+3 timeframe was used in this study. A model of this aircraft was constructed in FLOPS. Two versions of this aircraft were created. The TeDP system is integrated into the first version. The resulting TeDP/HWB combination, seen in Figure 2, is referred to as the N3-X. The second version has two ultra high bypass (UHB) geared turbofans mounted on pylons on the upper surface. The UHB turbofan is assumed to have the same component efficiencies and material temperature

limits as assumed for the TeDP. The UHB/HWB configuration, seen in Figure 3, is very similar to the Boeing/NASA N2A and so is referred to as the N3A. Engine simulations of the TeDP and the UHB were constructed using the NPSS

Figure 2 N3-X FLOPS Model

program. Engine performance from the TeDP and UHB simulations are then input into the FLOPS models of the vehicles to allow vehicle sizing and mission analysis to be performed.

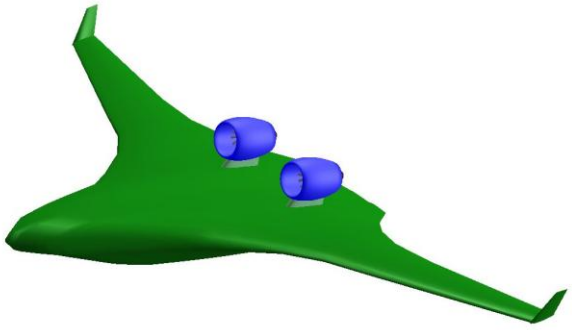

Figure 3 N3A FLOPS Model

N3-X and N3A Thrust Requirements

The aircraft thrust requirements for the N3-X and N3A are defined at two flight conditions; rolling take-off (RTO) at sea level, Mach 0.25, ISA+27R hot day, and the aerodynamic design point (ADP) at 30000 ft, Mach 0.84, ISA standard day. Even with the same technology assumptions for the turbomachinery, the differences in configuration between the N3-X and N3A engines yield a considerable difference in installed specific fuel consumption. The result is very different gross take-off weights and thus thrust levels for N3 aircraft with the two engine types.
Table 2 gives the uninstalled thrust required for the N3A and N3-X. These thrust values were used to size the two propulsion systems.

The nature of the TeDP configuration is such that there is very little installation drag. This is because the only extra external wetted area over the basic airframe is the sides of the propulsor array and the turbogenerator nacelle. The top of the propulsor nacelle has the same wetted area as the aircraft fuselage section that it covers. Thus no installation drag penalties were assessed against the TeDP on the N3-X configuration. The UHB, however, does have installation drag

Configuration	Flight Condition	Uninstalled Thrust lbf(kN)
N3A	RTO	78766 (350.37)
	ADP	25378 (112.89)
N3-X	RTO	54888 (244.15)
	ADP	19293 (85.82)

Table 2 N3A and N3-X Uninstalled Thrust Requirements

associated with the nacelle and pylon. The result is that comparing uninstalled performance of the two engine types would be misleading. Thus performance of the two engine configurations can be compared only on an installed basis.

Boundary Layer Conditions

A detailed understanding of the inlet flow field is critical to correctly estimating the performance of a BLI propulsion system as demonstrated by the authors in prior work[14]. The results of a three-dimensional (3-D) computational fluid dynamics (CFD) simulation of the closely related N2A-EXTE aircraft by Friedman[15] was used to estimate the boundary layer Mach number and total pressure profiles at a range of percent chord locations along the centerline. The N2A-EXTE represents an extension of the tail region by about 200 inches to a chord length of 1800. This was done to provide additional aft fuselage for noise shielding. The N3-X does not include this

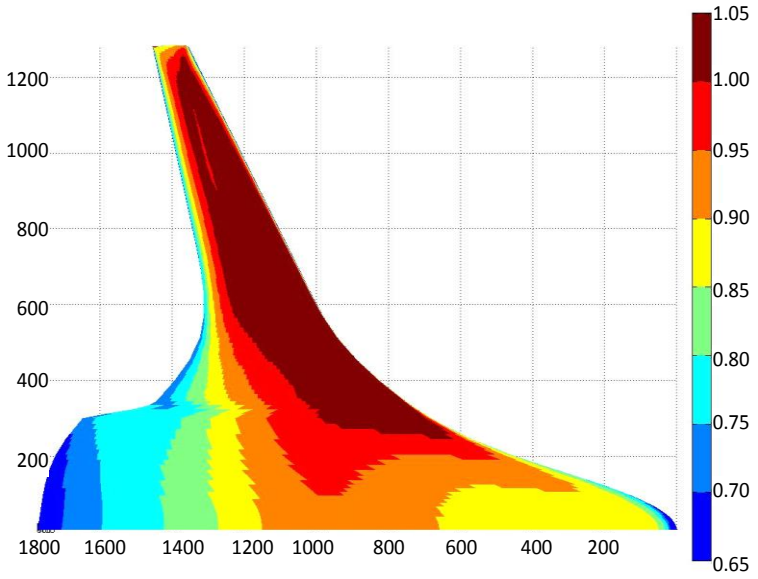

Figure 4 N2A-EXTE Upper Surface Isentropic Mach Number Distribution

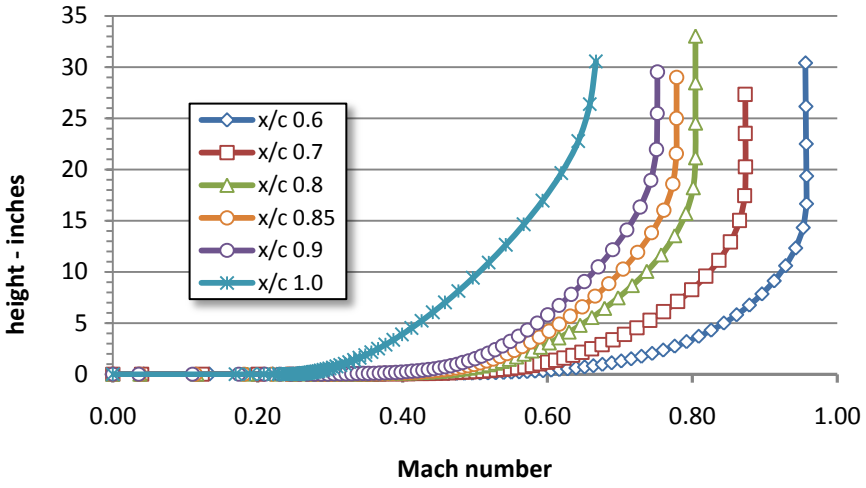

Figure 5 N2A-EXTE Centerline Boundary Layer Mach Number Profiles

extension. However, the differences are small enough that it was judged that the boundary layer shape and height would be the same on the two aircraft at the same percent chord locations. Figure 4 shows the inviscid Mach numbers at the top of the boundary layer for the top of the aircraft. Figure 5 shows the Mach number profiles for a range of percent chord locations along the centerline of the N2A-EXTE. Sizing the propulsors around a 1.3 fan pressure ratio resulted in the inlet plane being located at the 85% chord location. Therefore the boundary layer profile for this location was used to represent the boundary layer entering the propulsor inlets.

The velocity and density of the flow at each location in the boundary layer at the 85% chord location was used to calculate the mass flow per unit area at all values of height in the boundary layer. These mass flow rates were used to determine the mass-averaged Mach number and total pressure for a given inlet height. This was repeated for all heights to give curves of mass-average Mach number and total pressure versus inlet height. To extend the usage of these curves beyond the flight condition of the original CFD simulation, the curves were normalized by the freestream Mach number and total pressure at which the CFD was run. The resulting PtRatio and MNratio are given in Figure 6.

These two curves are central to estimating the effect of ingesting the boundary layer. When sizing the propulsors at the ADP flight condition the freestream Mach number and total pressure of 0.84 and 6.93 psia are used to unnormalize

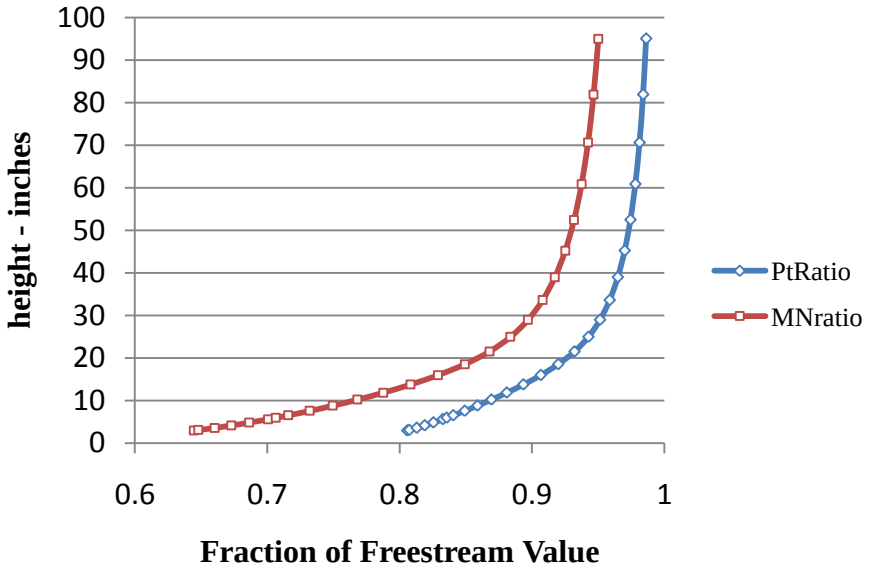

Figure 6 x/c = 0.85 Mass-avg PtRatio & MNratio

the curves. An estimate of the required inlet height is made and the mass-average Mach number for that height is used to determine the inlet mass flow. Also with the mass-averaged Mach number and total pressure the diffusion or ram drag resulting from the inlet is also calculated. With the inlet mass flow and total pressure the thrust produced by each propulsor can be calculated. This is compared to the required thrust, and if not equal then the inlet height is varied until they are.

A similar process is used in off-design calculations to determine the capture height of the inlet stream (assuming that the width of the inlet stream does not vary). If the capture height is less than the inlet height, then the mass-average inlet Mach number and total pressure decreases. Also when the capture height is less than the inlet height there is external diffusion sufficient to expand the flow from the capture height to the inlet height. Effects of the external diffusion on the flow field in front of the inlet are not captured at this time.

The benefit from BLI is captured in the reduced ram drag that results from the mass-average inlet velocity being lower than freestream velocity. The BLI benefit is higher at conditions, such as part power, where the capture height is less than the inlet height due to the continued decrease in average velocity with reduced capture height.

When the capture height is higher, then there is external acceleration to contract the flow down to the physical inlet height. The external acceleration causes a drop in the external static pressure. This suction effect along the trailing edge will enhance the circulation around the fuselage leading to an increase in the lift coefficient. Quantifying the change in the lift coefficient due to inlet suction and its impact on balance field length will be the subject of future analysis.

The wing-tip location results in freestream inlet conditions to the inlets of the turbogenerators, and so the propulsor inlet conditions have no effect on the turbogenerator performance.

Turbomachinery Design

The N+3 performance goals represent an extreme technical challenge. To assess the ability of the TeDP/HWB concept to reach the goal of 70% reduction in mission fuel burn, an optimistic approach to estimating the design parameters was taken to determine if the fuel burn goal was obtainable even with optimistic assumptions. All turbomachinery efficiencies, temperature limits and material assumptions

Componen	**Parameter**	**Design Value/Assumptions**
Inlet	Geometry	2-D "mailslot". Width equal to fan diameter plus spacing between adjacent fans. Height calculated from flow area divided by width.
	dP/P (throat to fan)	0.002
Fan	PR	1.30
	Adiabatic efficiency	0.9535
	Distortion efficiency penalty	0.01
	Design Tip Speed	883 ft/sec
Nozzle	Geometry	2-D low aspect ratio with variable exit area
	Cdth	0.997
	Cv	0.997

Table 3 Propulsor Design Parameters

Component	**Parameter**	**Design Value/Assumptions**
LPC & HPC	Polytropic efficiency	0.9325
HPC	Maximum exit total temperature (T3)	1810 R @ RTO, 1681 R @ ADP
LPC & HPC	Pressure Ratio (PR)	Total PR varied to equal max T3 with an equal Δh (enthalpy) split between compressors
Burner	Exit total temperature (T4)	3360 R @ RTO, 3260 R @ ADP
HPT & LPT	Polytropic efficiency	0.93
PT	Polytropic efficiency	0.924
Turbine material	Ceramic Matrix Composite (CMC)	Uncooled for all hot section components including burner liner, and turbine stators and rotors with 3460 R max material temperature
HPT	Non-chargeable disk cooling	4%
LPT	Non-chargeable disk cooling	2%
PT	chargeable disk cooling & cavity purge	1%
Nozzle	PRdes	1.6 @ 30k/MN0.84 ADP
	PRmin	1.01

Table 4 Turboshaft Engine Design Parameters

used in the TeDP system were applied to UHB geared turbofan engine as well.

The design assumptions for the propulsor are given in Table 3. The fan efficiency and design tip speed were first obtained from a NASA N+1 study of engines for single-aisle transports.[16] Analysis by Tillman[10] indicates that with optimization of the inlet geometry the distortion impacts of BLI can be limited to efficiency penalties of 1% to 2%. The baseline fan efficiency represents N+1 technology, so we assessed only a 1% efficiency penalty. The same optimization that reduced the impact on efficiency also reduced the internal total pressure loss of the embedded inlet to 0.2%-0.3%. The relatively low fan pressure ratio necessitates a variable area propulsor nozzle.

The segmented 2-D "mail-slot" nozzle allows the upper surface of the nozzle to be simply hinged to provide the necessary variability.

Table 4 contains the design efficiencies and temperatures for the turbogenerator. The pressure ratio split between the low pressure and high pressure compressors was varied such that there was an equal enthalpy rise across each compressor. NASA materials roadmaps for ceramic matrix composites (CMC) anticipate a maximum material temperature of 3460R. With this material temperature limit, turbine blade cooling is unnecessary. The burner exit pressure was set at 3360R to give a 100R factor of safety. Some cooling flow is still required to cool the turbine rotor disks and for cavity purge. The nozzle pressure ratio was set to yield minimum thrust at cruise. The result is that more of the energy in the gas stream is extracted by the power turbine and directed to the generator and less is left in the exhaust flow. The result is a lower exhaust gas velocity from the turbogenerator, especially at the RTO condition where noise is critical. If the turbogenerator noise is found to be an issue in meeting the N+3 noise goal a possible option is a variable area turbogenerator exhaust nozzle. This would allow the nozzle area to be increased at high power settings to further increase the pressure ratio across the power turbine and decrease the nozzle exhaust further from what is possible with a fixed area nozzle. At cruise conditions the nozzle area would be reduced to produce an optimal amount of thrust directly from the turbogenerators.

Electrical Power System

In the following sections the components required in a superconducting electrical power system are listed and briefly discussed. The methods underlying this section are the same as presented in Brown's paper on weights and efficiencies of electric components of a turboelectric aircraft propulsion system[17]. That same analysis has been repeated here for the current motor and generator power levels of 4000 hp and 30000 hp respectively. The resulting weights and efficiencies of each of the electrical components is presented in Table 7 for magnesium di-boride (MgB_2) and in Table 8 for bismuth strontium calcium copper oxide (BSCCO). The power levels used to size the electric system are those needed at the rolling take off (RTO) flight condition. This is done because the electrical portion of the system must be sized to handle the highest power transmitted, which is at take-off. . The turbomachinery portions of the propulsion system are sized at the aerodynamic design point (ADP).

Fully Superconducting Generator

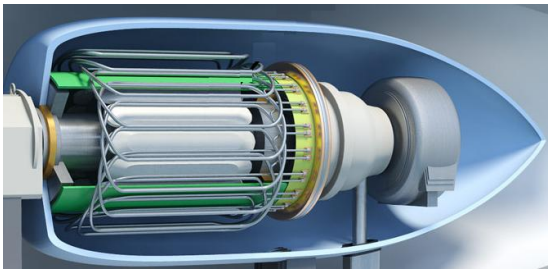

Figure 7 Schematic Drawing of a Fully Superconducting Electric Machine

This study assumes that the required power density of the motors and generators is obtained from wound rotor synchronous machines with superconductor windings on both rotor and stator. The state-of-the-art of superconducting machines has been reviewed in various papers cited in reference 17. Such a machine is depicted schematically in Figure 7. The stator windings deliver AC power to be rectified and transmitted as DC power by superconducting transmission lines. The high power electrical components all operate at cryogenic temperatures without any electrical leads between cryogenic temperatures and room temperature.

The windings in the stator of the generator are subject to alternating magnetic fields and alternating currents (AC), and therefore suffer superconducting AC losses. To keep the required cooling capacity within acceptable bounds, these stator conductors must be carefully engineered to reduce the AC losses. This can be achieved by using small diameter wire with fine superconducting filaments embedded in a resistive metallic matrix. The required filament size presently appears achievable only for the superconductor MgB_2. A 2009 NASA Small Business Innovation Research (SBIR) contract conducted by Hyper Tech Research, Inc[18] examined the production of MgB_2 suitable for use in turbo-electric aircraft propulsion system. Figure 8 shows the cross section of their interim design. Unfortunately, the critical temperature (the highest temperature at which it is superconducting) for MgB_2 is only 39K, and it must operate below 30K to yield a useful current density. This increases the weight of the required cryocooler. Even though BSCCO cannot currently be formed with acceptable AC losses, a future development is assumed that will make it possible. Motors and generators with a hypothetical fine-wire BSSCO are included in this study. The superconductor yttrium barium copper oxide (YBCO) was not considered for this application because no concept for suitably low AC loss has yet been advanced for this material.

Figure 8 Low-AC Loss Superconducting Configuration

Note that the generator shaft speed can be chosen to match the optimum speed of the power turbine in the turbine engine. that speed can be high enough to reduce the power turbine weight substantially below the value required for a direct drive large fan. Thus electric drive provides the same advantage with respect to turbine weight as a planetary gear box.

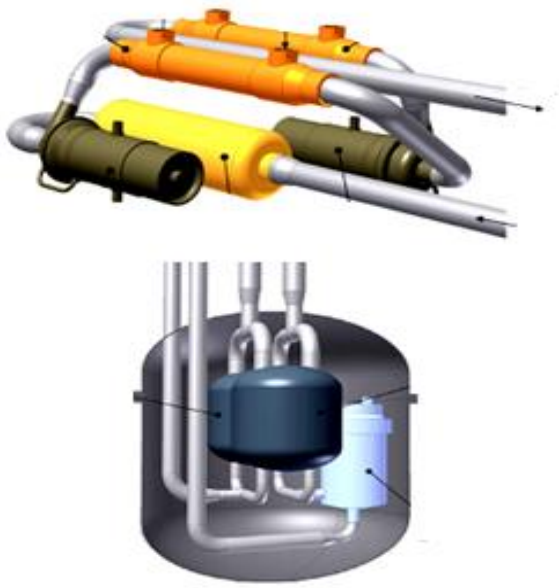

Figure 9 Turbo-Brayton Cryocooler

Cryocoolers

A cryocooler is a refrigerator that produces very low temperatures. The superconducting devices used in the TeDP system require temperatures between 20K and 65K. A 2009 NASA SBIR study conducted by Creare[19] produced a preliminary design of a turbo-Brayton cryocooler, depicted in Figure 9, which meets our current weight goal of 5 lb/hp-input. This is about $1/6^{th}$ the weight of the best present coolers and is expected to achieve the same 30% of Carnot efficiency attained by the best current technology coolers. A more appropriate functional dependence of the weight on the input power (instead of simple proportionality) is not yet within our modeling capability.

The cryocoolers are driven by their own electric motors, which are included in the weight estimate. The power to drive the cryocoolers comes from the turbogenerators. Thus the power losses in the superconducting devices and the inverters plus the power to the cryocoolers

represent the total transmission power loss. The amount of power required by the cryocoolers depends on the operating temperature of the device being cooled (the source temperature) and the temperature at which heat is being rejected (the sink temperature). The larger the difference between the source and sink temperatures, the greater the cryocooler power required. It is for this reason that the cryocooler power and weight is higher for MgB_2 based devices which operate below 30K than for BSCCO based devices which operate near 50K.

Liquid Hydrogen Cooling

Liquid hydrogen was examined as an alternate to cryocoolers to cool the superconducting motors, generators and transmission lines as well as the cryogenic inverters. Liquid nitrogen does not present an alternative. This is because even though the BSCCO material has a critical temperature above the boiling point of liquid nitrogen, the critical current density at liquid nitrogen temperature is too low to yield motors, generators and transmission line with weights useful in an aircraft application. The critical current density rises sharply with decreasing temperature. With a boiling point of 20.4K at ambient pressure, liquid hydrogen provides an operating temperature that yields very high current densities, resulting in smaller and lighter motors, generators and power lines. Liquid hydrogen can also directly cool MgB_2 based machines, which need to operate at 30K or less.

In the refrigerated system, cryocoolers represent the largest power "loss" in the transfer of power from the power turbines to the fans. The use of liquid hydrogen eliminates this particular loss and substantially increases the power transmission efficiency. The hydrogen cooling flow rate required is calculated by assuming that hydrogen boils at constant temperature in the AC stator with the cold gas that is evolved cooling the nearly lossless DC rotor. The hydrogen gas from the motors then travels to the associated inverters to cool those devices. If the heat capacity of the hydrogen flow required to cool the motor is not sufficient to cool the inverter, then additional liquid hydrogen is introduced to remove the remaining heat with a combination of latent heat and sensible heat capacity.

After serving as a coolant, the hydrogen, with a lower heating value of 51585 BTU/lb, is compressed and introduced to the burner of the turbogenerator where it replaces a portion of the jet fuel equal to approximately 2.8 times the mass of the hydrogen. The amount of hydrogen required is very small compared to the energy needed to propel the aircraft and so jet fuel still constitutes the majority of the fuel energy.

Superconducting Transmission Lines

The superconducting transmission line has not yet been studied in detail for this application. Many studies and demonstration projects for ground transmission lines for utility grids have been made or are under way. Either AC or DC transmission is possible. A 2006 Chinese test of a superconducting, 60 Hz AC cable was reported. The 3-phase cable carried 120MW (over twice the N3-X take-off power of 45 MW) and the mass of each phase was 9.2 kg/m[20]. Losses are only a few watts per meter. Superconducting cables typically operate at liquid nitrogen temperature, 77K. But cooling to approximately 55K, to match the motors and generators of the TeDP system, would increase the critical current density and allow about 3 times the power capacity for the same cable size. Pending detailed studies, a weight of 1000 lb for superconducting cables was added to the total electrical system weight. Transmission losses and environmental heat transfer combined are typically on the order of 5 W/m of cable length. In addition to its central task of carrying current, the transmission lines, which are built around a hollow core to carry a coolant for its own cooling, can also be used to carry coolant to motors or generators, avoiding a separate coolant line and allowing a central location for the cryocoolers or hydrogen tanks.

Fully Superconducting Motors

An electric machine can operate as either a motor or a generator. The superconducting motors were sized with the same sizing code and treated in exactly the same fashion as the generators. It was assumed that they are driven by cryogenically cooled inverters so that the

shaft speed of the fans can be varied independently of the generators. For the example aircraft, N3-X, of Fig. 1, fifteen motors of 4,000 hp each are required. With a maximum fan tip speed of 883 ft/s (for a 1.3 FPR) and a calculated fan diameter of 43 inches, the fan motor shaft speed is calculated to be 4500 rpm.

Cryogenic Inverters

Inverters convert direct current to alternating current of any desired frequency and therefore can drive a motor at a variable speed. Inverters allow the fan speed to be independent of the engine's power shaft speed, in effect acting as a variable ratio gear box. This is a key factor in allowing all propulsors to continue to operate in the event that a turbogenerator fails. In that situation the propulsor speeds would drop to the point where the power demand equals the power from the remaining turbogenerator. The remaining turbogenerator, meanwhile, would

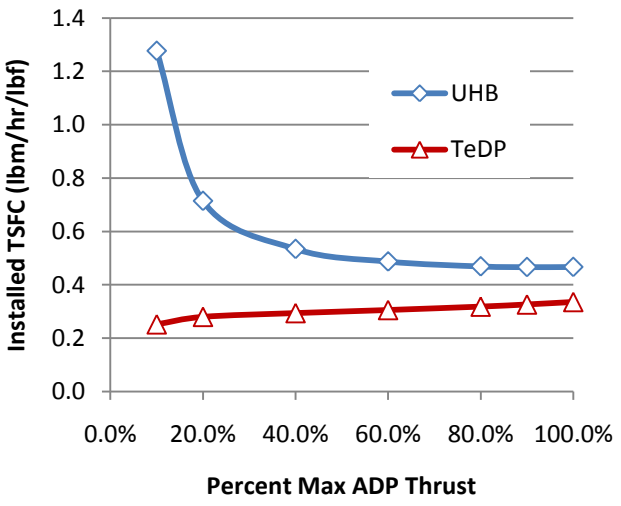

Figure 10 UHB & TeDP Installed TSFC Vs Percent of Maximum Thrust at ADP

have to maintain or even increase speed and power output. Various factors related to the inverters are discussed in reference 17, including the higher efficiency and lower weight of cryogenically cooled inverters. These advantages hold even when the required cryocooler weight and efficiency is taken into account. A 2010 NASA SBIR has predicted that a cryogenic inverter could attain a specific power of 15 hp/lb, including the cryocooler[21]. This specific power is used here to estimate the weight of the inverters for the given power level. At cruise power levels the inverter efficiency could be as high as 99.93% for the inverter itself. Including power to drive a cryocooler to provide the necessary temperature the combined efficiency is still 99.5%. The efficiency at takeoff power levels would be about 0.25% lower, but the duration of takeoff is short, so the impact on total fuel burn is not significant.

Analysis and Results

Engine Performance Table 5 and Table 6 compare the performance of the TeDP system to the performance of the geared UHB turbofan and the NASA developed Pax300 direct drive turbofan[22]. The Pax300 model is similar to the GE90-115B present on the reference aircraft, the Boeing B777-200LR. It is included here to give a current technology metric. The UHB and TeDP engines were iterated with the FLOPS models of the N3A and N3-X aircraft to determine the fuel load necessary to perform the reference mission and thus determine both the empty and gross take-off vehicle weights. The low fuel consumption of the TeDP resulted in a smaller fuel load and thus a smaller vehicle that required less thrust that in turn reduced the size of the TeDP engine.

Both the UHB and TeDP engines are sized to a fan pressure ratio (FPR) of 1.3 at the aerodynamic design point (ADP) and a T3 of 1810R and T4 of 3360 R at the rolling take-off (RTO) flight conditions while meeting the thrust required at both flight conditions. The thrust lapse rates with altitude and speed for both the UHB and the TeDP cycles were such that engines were designed to provide more thrust at the ADP point than the aircraft required in order to match the thrust required at the RTO flight condition. The UHB is capable of 5% more thrust at the ADP flight condition than the N3A requires, while the TeDP system is capable of 20% more thrust.

Requiring the TeDP system to be oversized by 17% at the ADP point would ordinarily cause

the cruise fuel efficiency to be penalized since standard engine behavior is for the TSFC to increase with decreasing thrust for a given flight condition. However, the TeDP does not exhibit this behavior. Figure 10 compares the TSFC versus percent power trends for the UHB and TeDP engines. The UHB engine exhibits the standard "power-hook" trend of small increase in TSFC from 100% to 80% thrust with ever faster increase in TSFC with further throttling. The TeDP engine displays a completely different trend. For the TeDP the TSFC declines in a continuous manner such that the lowest TSFC is actually at idle. At 83% of maximum thrust, the TSFC of the TeDP is 5% lower than at maximum thrust. The reason for this unusual trend is that the effect of BLI increases at part power.

Table 7 and Table 8 present weights and efficiencies of the major electrical components of the TeDP system on the N3-X aircraft. A generator with its cooler was optimized with respect to several design parameters to minimize the combined weight. A motor with its cooler was separately optimized in the same way.

RTO	Reference Engine	N3A	TeDP (Cryo)	TeDP (LH2)
Altitude (ft)	0	0	0	0
Mach number	0.25	0.25	0.25	0.25
dTs (R)	27	27	27	27
Pt (ambient)	15.35	15.35	15.35	15.35
MN (capture)	0.25	0.25	0.233	0.233
Pt (capture)	15.35	15.35	14.94	14.94
T3 (R)	1673	1803	1791	1789
T4 (R)	3296	3360	3358.4	3356
Fn (Installed)	161215	78249	54888	54882
W_{fuel} (lb/hr)	63134	20177	13807	11867
TSFC (installed) (lbm/hr/lbf)	0.3919	0.2578	0.2515	0.2162
W_{air} (lb/s)	6503	6539	4940	4944
BPR	8.8	29.5	32.7	34.2
FPR	1.49	1.2	1.2	1.2
OPR	43.1	57.4	56.1	55.8
V_{amb} (ft/s)	286.3	286.3	286.3	286.3
$V_{capture}$ (ft/s)	286.3	286.3	267.1	267.1
V_{bypass} (ft/s)	923	665	618.6	618.6
V_{core} (ft/s)	1126	898	817	818
$\eta_{Propulsive}$ (bypass)	47.3%	60.2%	64.6%	64.6%
$\eta_{Propulsive}$ (core)	40.5%	48.3%	52.8%	52.8%
$\eta_{Propulsive}$ (avg)	46.7%	59.8%	64.3%	64.3%
Fan Diameter (in)	128	150	41	41
A_{fan} (vehicle) (in2)	25736	35249	19746	19784

Table 5 Rolling Take-off (RTO) Engine Performance

The total electrical system weights are for a system with 15 propulsors and 2 turbogenerators. Each propulsor has one motor and one inverter. Each turbogenerator has one generator. The transmission line weight represents the estimate of transmission line weight for the entire aircraft. The weight for the cyrocooled system includes the weights of the motor, inverter and generator cryocoolers. The weight of the LH2 cooled system in these tables excludes the weights of the cryocoolers, but does not include an estimate of the hydrogen tankage weight, which dependents on hydrogen required for the design mission. The weight of the hydrogen coolant itself is included in the fuel weight rather than the electrical system weight.

The operating temperature for MgB_2 based devices of less than 30K results in higher cryocooler power and larger, heavier

ADP	Reference Engine	N3A	TeDP (Cryo)	TeDP (LH2)
Altitude (ft)	30000	30000	30000	30000
M (amb)	0.84	0.84	0.84	0.84
dTs (R)	0	0	0	0
Pt (ambient)	6.93	6.93	6.93	6.93
M (capture)	0.84	0.84	0.735	0.735
Pt (capture)	6.93	6.93	6.48	6.48
T3 (R)	1510	1670	1603	1603
T4 (R)	3029	3212	3049	3051
Fn (Installed)	55697	24173	19293	19293
W_{fuel} (lb/hr)	31495	11281	6659	5673
TSFC (installed) (lbm/hr/lbf)	0.5780	0.4667	0.3451	0.294
W_{air} (lb/s)	3501	3485	2503	2505
BPR	8.5	27.2	30.5	31.7
FPR	1.587	1.290	1.26	1.26
OPR	43.1	71.1	64.1	64
V_{amb} (ft/s)	835.8	835.8	835.8	835.8
$V_{capture}$ (ft/s)	835.8	835.8	742.3	742.5
V_{bypass} (ft/s)	1040	1006	986.8	986.8
V_{core} (ft/s)	1587	1418	1164	1169
$\eta_{Propulsive}$ (bypass)	89.1%	90.8%	96.7%	96.7%
$\eta_{Propulsive}$ (core)	69.0%	74.2%	87.7%	87.4%
$\eta_{Propulsive}$ (avg)	87.0%	90.2%	96.4%	96.4%

Table 6 Aerodynamic Design Point (ADP) Engine Performance

cryocoolers than are required for BSCCO based systems which operate at 50K or more. With a boiling point at atmospheric pressure of 20.4K, liquid hydrogen represents an attractive alternative to cryocoolers for MgB_2 based devices. The advantages of hydrogen are fourfold.

First, the 6064 lbs weight of the cryocoolers listed in
Table 7 is eliminated. Partially offsetting this is the need to carry cryogenic tanks to hold the hydrogen. Technology for hydrogen tanks that are one third to one half the weight of the hydrogen contained is being explored.[23] About 2370 lbs of liquid hydrogen is required to cool the MgB_2 system for the reference mission. This would require a hydrogen tank weighing about 1185 lbs, for a net empty weight reduction of 4861 lbs, compared to the cryocooled MgB_2.

Second, the hydrogen can be used as fuel after it is used as a coolant. Hydrogen has a lower heating value (LHV) of 518585 BTU/lb while jet fuel has a LHV of 18580 BTU/lb. Thus one pound of hydrogen can replace about 2.8 pounds of jet fuel. Thus the 2370 lbs of hydrogen replaces 6615 lbs of jet fuel for a net benefit of 4245 lb reduction in total fuel

Third, the efficiency of transferring power from the engines to the fans rises from 97.75% to 99.88% without power being consumed by the cryocoolers. This 2.1% increase in transmission efficiency will translate directly into reduction in total fuel weight.

Fourth, the necessary hydrogen can be generated from non-carbon emitting sources of power. Also hydrogen generators located at the airport can serve as load of last resort for renewable power sources like wind, solar, or wave for times when more power is being generated than can otherwise be used. Coordination between airports and local electrical companies can use the hydrogen generation systems to help balance the load on the entire electrical grid in a way that provides benefits to both parties.

The impact of change in efficiency plus the effect of higher LHV reduces the fuel weight a total of 6050 lbs compared to an MgB_2 system

		MgB_2	
Component	Weight (lb)	Efficiency (%)	Specific Power (hp/lb)
Generator,	1184	99.98%	25.3
Generator Cooler	1005		
Generator with Cooler	2189	99.28%	13.7
Transmission line	1000		
Inverter	200	99.93%	20
Inverter Cooler	67	99.57%	
Inverter with Cooler	267	99.50%	15
Motor	314	99.97%	13.4
Motor Cooler	202		
Motor with Cooler	516	98.95%	7.8
Total -Cryocooled	**17123**	**97.75%**	3.5
Total - LH2 Cooled	**11078**	**99.88%**	5.4

Table 7 MgB_2 **Based Electrical System Weights and Efficiencies.**

		BSSCO	
Component	Weight (lb)	Efficiency (%)	Specific Power (hp/lb)
Generator,	954	99.93%	31.4
Generator Cooler	580		
Generator with Cooler	1534	99.55%	19.6
Transmission line	1000		
Inverter	200	99.93%	20
Inverter Cooler	67	99.57%	
Inverter with Cooler	267	99.50%	15
Motor	298	99.94%	13.4
Motor Cooler	93		
Motor with Cooler	391	99.48%	10.2
Total -Cryocooled	**13938**	**98.54%**	4.3
Total - LH2 Cooled	**10378**	**99.80%**	5.8

Table 8 BSCCO Based Electrical System Weights and Efficiencies.

with cryocooling. The combination of lower empty weight and lower fuel weigh means that in a MgB_2 system hydrogen cooling can reduce the TOGW 10900 lbs compared to a system with cryocooling.

The BSCCO system summarized in Table 8 can operate at 50K. This higher source temperature for the cryocooler reduces the weight of the cryocoolers for the motor and generator by about half compared to the MgB_2 system. While hydrogen cooling would have the same advantages with the BSCCO system as the MgB_2 system, the impact wouldn't be as significant. For this reason, the N3-X with cryocooling uses the weights and efficiencies defined for BSCCO based motors and generators.

The TeDP systems of the N3-X vehicle, even with the additional weight of the electrical transmission system, are lighter than the total propulsion system weight of the pylon mounted UHB engine on the N3A with the same assumed technology level. Contributing to the lower weight is the improved specific fuel consumption of the TeDP relative to the UHB resulting in less fuel burn, which allowed the N3-X to be smaller and lighter than the N3A aircraft. This in turn reduced the thrust required of the TeDP engine, allowing the engine to be made smaller. The end result is that the smaller fan area (spread over 15 small fans rather than 2 large fans) and smaller core engines reduced the turbomachinery weight 13552 lbs. The embedded design of the TeDP saves 10348 lbs in the inlet, nacelle and bypass nozzle weight and eliminates the pylon entirely. The

Engine Weights *(total for the vehicle)*	Reference Engine (lb)	N3A (lb)	TeDP (Cryo) (lb)	TeDP (LH2) (lb)
Turbomachinery (core and fan)	33622	28887	15335	15335
Gearbox/Electrical	0	592	13938	11841
Inlet/Nacelle/Nozzle/Pylon	8829	13377	3029	3029
Propulsion System Total Weight	**42451**	**42856**	**32302**	**30205**

Table 9 Engine weight comparison

	Reference Aircraft (lb)	N3A (lb)	N3-X (Cryo) (lb)	N3-X (LH2) (lb)
Empty Wt	340800	285800	26780	267400
Payload Wt	118100	118100	118100	118100
Total Fuel Wt	309800	147200	93400	88000
Block Fuel Wt	279800	133700	83500	78500
Reduction in Block Fuel		**52.2%**	**70.2%**	**71.9%**
TOGW	**768700**	**551000**	**479300**	**473500**

Table 10 Aircraft Weight Comparisons and Percent Block Fuel Burn Reduction

large differences in the configuration of the two engines make it difficult to single out aspects that lead to this difference in weight. Aspects, such as the 2-D nozzle of the TeDP propulsors that allow a variable fan nozzle area to be accomplished with a simple hinged flat nozzle flap, certainly contribute to the weight difference. More detailed analysis will be needed to understand the differences.

The end result of this analysis is that the N3-X with a TeDP system was able to meet the SFW project goal of 70% mission fuel burn reduction. Figure 11contains the decomposition of the mission fuel burn reduction for the N3A and the N3-X with cryocooling and liquid hydrogen cooling giving the fuel burn reduction attributed to each technology applied.

Conclusions

The hybrid wing body (HWB) aircraft combined with turboelectric distributed propulsion (TeDP) system is able to reduce the mission fuel burn by 70%-72% from that of a B777-200LR-like vehicle (block fuel burn of 279800 lbs), without compromising payload, range or cruise speed. This is accomplished by using an electrical drive system that decouples the power producing parts of the system from the thrust producing parts of the system with only a relatively lightweight and flexible electric transmission lines connecting them. This freedom to configure and locate those two major portions of the propulsion system allowed each to be optimized for its task.

Fifteen propulsors were located in a continuous nacelle with 2-D “mail-slot” inlets and nozzles that covered the entire 60 foot span of the center body near the upper surface trailing edge of the N3-X aircraft. This maximized the amount of boundary layer that was ingested by the system. Despite the wide span of the total array, the aspect ratio of each individual propulsor inlet is only 2 to 1. The aspect ratio of each nozzle is a similar 2.7 to1. This allows short, minimal offset, low loss inlets and nozzles with only a fan and motor between. The short axial length of the propulsor allows placement of the inlet at the 85% chord location while still keeping the nozzle plane well forward of the trailing edge to retain the fuselage noise shielding benefit of the HWB configuration. Aft of the 80% chord location the inviscid portion of the inlet flow has less than freestream velocity

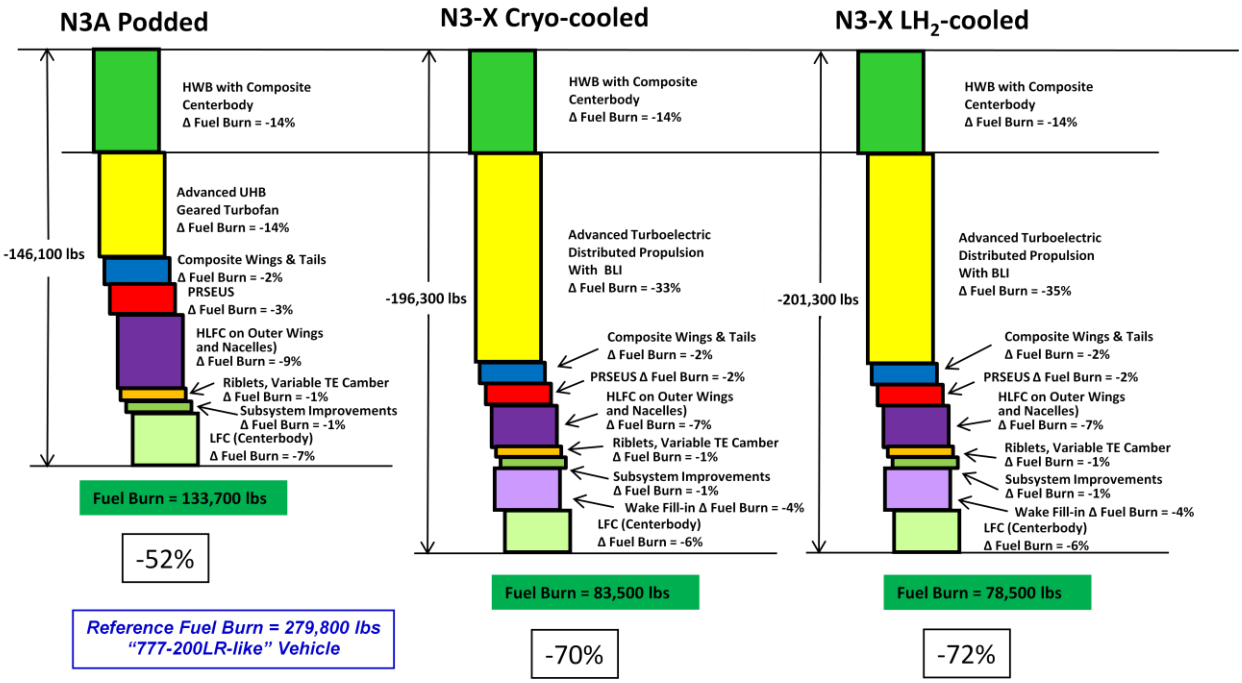

Figure 11 Fuel Burn Reduction Breakdown

due to diffusion on the aft portion of the HWB center body. The ability to keep the inlet aft of the 80% chord location allows the combination of BLI and aft diffusion to reduce inlet velocities further than just BLI alone would. This results in a total of 10% reduction in inlet velocity at the 85% chord location at the ADP flight condition.

Two large turbogenerators that produce the power to run the propulsors were located at the wing tips where they would receive undisturbed freestream air. The combination of the largest possible turboshaft engine size and a freestream inlet allowed the highest possible thermal efficiency for a given set of engine technology assumptions. However all of the thermodynamic advantage would be retained if the turbogenerator were moved to an inboard location, such as the wing root.

Many of the technical issues involving development of flight-weight superconducting motors, generators and transmission lines appear to be addressable and will benefit from very active research on both aerospace and terrestrial applications. The key area of investigation is development of AC tolerant stator designs, with MgB_2 currently the best candidate material. Preliminary research results in the areas of cryocoolers, refrigeration, and cryogenic power inverters show that target power to weight goals may actually be within reach of current technology. Liquid hydrogen cooling presents an alternative to mechanical refrigeration, and also has other advantages such high heating value which allows a single pound of hydrogen to displace nearly 3 pounds of jet fuel, reducing the mission fuel weight even further. The need to generate the hydrogen may offer synergies with renewable power sources such as solar and wind energy. The efficiencies afforded by electrical power transmission result in very significant fuel burn savings. So significant in fact that the resulting reductions in aircraft size and weight lead to TeDP engines that are lighter, with the weight of their electric system included, than the conventional pylon mounted turbofan engines, including nacelle and pylon, of the same technology level.

With the ability to meet the fuel burn goal established, analysis will continue to determine the fuel burn sensitivities to changes in the assumed technology levels. This will indentify

both the technologies to which fuel burn is most sensitive and the threshold values of those technologies required to maintain the 70% fuel burn reduction. A noise analysis will also be performed to determine the aircraft noise with respect to the N+3 noise reduction goal of -71 db. Lastly, the effect on the lift coefficient of the upper surface suction produced by the propulsor array, and the impact that has on balance field length, will be determined.

Acknowledgements

The authors would like to thank Mr. Michael Tong, our "fifth" author, for taking one for the team. We would like to thank Dr. Rubén Del Rosario for his encouragement and advocacy as we traveled through undiscovered territory while developing concepts for this new class of engines. We would also like to thank Dr. Richard Wahls, Mr. Gregory Follen, Mr. William Haller and the rest of the SFW management team for their assistance and guidance; Mr. George Stefko for his enthusiasm and advocacy. And we would like to thank Dr. Fayette Collier for his leadership when we started looking at the seemingly impossible possibility of electric distribution of main propulsion power in large transport class aircraft.

References

[1] NASA Research and Technology Program and Project Management Requirements, NASA Procedural Requirements 7120.9. Appendix J. Technology Readiness Levels (TRLs), February 05, 2008

[2] Greitzer, Edward M., et al, "N3 Aircraft Concept Designs and Trade Studies," NASA Contractor Report CR-2010-216794, Volume 1 and 2, , 2010

[3] Bruner, Sam, et al., "NASA N3 Subsonic Fixed Wing Silent Efficient Low-Emissions Commercial Transport (SELECT) Vehicle Study," NASA Contractor Report CR-2010-216798, 2010

[4] Bradley, M. and Droney, C, "Subsonic Ultra Green Aircraft Research: Phase I Final Report", NASA Contract Number NNL08AA16B, 2010

[5] DAngelo, Martin M., et al., "N3 Small Commercial Efficient and Quiet Transportation for Year 2030-2035," NASA Contractor Report CR-2010-216691, 2010

[6] McCullers, L. A.: "FLOPS Weight Module Documentation, Wate.doc," FLOPS Users Manual, updated April 2008

[7] NPSS User Guide Software Release: NPSS_1.6.5

[8] Liebeck, R., "Design of the Blended Wing Body Subsonic Transport", *Journal of Aircraft*, Vol. 41, No. 1, Jan-Feb. 2004. pp. 10-25

[9] Thomas,R, Burley, C., Olson, E., "Hybrid Wing Body Aircraft System Noise Assessment With Propulsion Airframe Aeroacoustic Experiments", AIAA-2010-3913, 2010.

[10] Tillman, Greg, et all, "Robust Design for Embedded Engine Systems – BLI Inlet and Distortion-Tolerant Fan Design", NASA Contract Number NNC07CB59C, 2010

[11] Patterson, J.C., Flechner, S.G., "An Exploratory Wind-Tunnel Investigation of the Wake Effect of a Panel Tip-Mounted Fan-Jet Engine on the Lift-Induced Vortex", NASA TN D-5729, May, 1970

[12] Kawai, Ron, et al, "Acoustic Prediction Methodology and Test Validation for an Efficient Low-Noise Hybrid Wing Body Subsonic Transport", NASA Contract Number NNL07AA54C, 2008

[13] de la Rosa Blanco, E., Hall, C., Crichton, D., "Challenges in the Silent Aircraft Engine Design", AIAA-2007-454, 45th AIAA Aerospace Sciences Meeting in Reno, NV, January 8, 2007

[14] Felder, J, Kim, H. D., Brown, G., Chu, J. "An examination of the Effect of Boundary Layer Ingestion on Turboelectric Distributed Propulsion Systems", AIAA-2011-0300, 49th AIAA Aerospace Sciences meeting in Orlando, FL, January 4, 2011

[15] Friedman, D., "Aerodynamic Prediction Methodology and Test Validation for an Efficient Low-Noise Hybrid Wing Body Subsonic Transport". NASA Contract NNL07AA54C, 2nd Annual Review, NASA Ames Research Center, January 20, 2010

[16] Guynn, M. D., et. al., "Engine Concept Study for an Advance Single-Aisle Transport", NASA TM-2009-215784

[17] Brown, G. V., "Weights and Efficiencies of Electric Components of a Turboelectric Aircraft Propulsion System", AIAA-2011-0225, presented at 49th AIAA Aerospace Sciences meeting in Orlando, FL, Jan 4-7, 2011

[18] "Low AC-Loss Magnesium Diboride Superconductors for Turbo-Electric Aircraft Propulsion Systems", NASA 2009 Phase 1, SBIR, NNX09CC75P, Hyper Tech Research, Inc.

[19] "Thermal Management System for Superconducting Aircraft", NASA 2009 Phase 1 SBIR, NNX09CC77P, Creare Inc.

[20] Xi, H.X., Gong, W.Z., Zhang, Y., Bi, Y.F., Ding, H.K., Wen, H., Hou, B., Xin, Y., "China's 33.5 m, 35 kV/2 kA HTS AC Power Cable's Operation in Power Grid", Physica C, 445–448 (2006) 1054–1057

[21] "Lightweight, Efficient Power Converters for Advanced Turboelectric Aircraft Propulsion Systems", Final Report, NASA 2010 Phase 1 SBIR, NNX10CC71P, MTECH Laboratories, LLC, July 29, 2010

[22] Jones, S., NASA GRC Reference model for 90000 lb thrust class direct-drive turbofan, 2011

[23] Snyder, C, et al, "Propulsion Investigation for Zero and Near-Zero CO_2 Emissions Aircraft", NASA/TM-2009-215487, May, 2009